
Kernel-SSL: Kernel KL Divergence for Self-Supervised Learning

Yifan Zhang*

IIIS, Tsinghua University
zhangyif21@mails.tsinghua.edu.cn

Zhiquan Tan*

Department of Math, Tsinghua University
tanzq21@mails.tsinghua.edu.cn

Jingqin Yang*

IIIS, Tsinghua University
yangjq21@mails.tsinghua.edu.cn

Yang Yuan†

IIIS, Tsinghua University
Shanghai Artificial Intelligence Laboratory
Shanghai Qi Zhi Institute
yuanyang@tsinghua.edu.cn

Abstract

Contrastive learning usually compares one positive anchor sample with lots of negative samples to perform Self-Supervised Learning (SSL). Alternatively, non-contrastive learning, as exemplified by methods like BYOL, SimSiam, and Barlow Twins, accomplishes SSL without the explicit use of negative samples. Inspired by the existing analysis for contrastive learning, we provide a reproducing kernel Hilbert space (RKHS) understanding of many existing non-contrastive learning methods. Subsequently, we propose a novel loss function, Kernel-SSL, which directly optimizes the mean embedding and the covariance operator within the RKHS. In experiments, our method Kernel-SSL outperforms state-of-the-art methods by a large margin on ImageNet datasets under the linear evaluation settings. Specifically, when performing 100 epochs pre-training, our method outperforms SimCLR by 4.6%³.

1 Introduction

Self-supervised learning (SSL) has achieved remarkable performance on various tasks like image classifications and segmentations and even outperforms the supervised counterparts [10, 9, 36, 75, 6]. Contrastive learning is an important type of self-supervised learning methods. For example, SimCLR [10] proposes to use InfoNCE [46] loss to do contrastive self-supervised learning, and has been proved to exactly perform spectral clustering on similarity graph [56]. Spectral contrastive loss [21] is a variant of SimCLR and also has been proven to be doing spectral clustering under similar settings. The empirical success of contrastive learning has spurred a number of theoretical explorations into the contrastive loss [2, 22, 63, 64, 33, 69, 45, 29, 58, 27].

Recently, many researchers have proposed to do non-contrastive self-supervised learning without explicit negative samples using various different losses (BYOL [19], SimSiam [11], Barlow Twins [75], VICReg [6], MEC [38], etc). Many theoretical studies have also paid attention to the intrinsic mechanism behind non-contrastive SSL methods. For example, Garrido et al. [18] established the duality between contrastive and non-contrastive methods, and Balestriero & LeCun [5] unveiled the links of SimCLR, Barlow Twins and VICReg to spectral methods.

*Equal Contribution.

†Corresponding Author

³The code is available at <https://github.com/yifanzhang-pro/Kernel-SSL>.

From a kernel perspective, we provide a unified understanding of non-contrastive learning. Specifically, we generalize Wang & Isola [68]’s work on understanding contrastive representation learning, and propose the kernel alignment and kernel uniformity framework for Self-supervised Learning, directly optimizing mean embedding and covariance operator in reproducing kernel Hilbert space (RKHS). Additionally, we introduce innovative metrics to measure dimensional collapse, thereby quantifying intra- and inter-class effective ranks for diverse SSL methods.

In experimental evaluations, our method Kernel-SSL outperforms state-of-the-art methods (SimCLR, BYOL, SimSiam, Barlow Twins, VICReg) by a large margin on ImageNet datasets, especially under linear evaluation settings, our method uses only 100 epochs pre-training can outperform SimCLR 100 epochs pre-training by 4.6%, as demonstrated in Figure 1.

2 Related Work

Contrastive and non-contrastive SSL approaches Contrastive and non-contrastive self-supervised learning methods learn representations based on diverse views or augmentations of inputs, and they do not rely on human-annotated labels [10, 26, 72, 59, 11, 17, 4, 46, 73, 24, 43, 8, 21, 9, 36, 75, 66, 6, 60, 50, 15]. These representations can be used for various of downstream tasks, achieving remarkable performance and even outperforming supervised feature representations.

Theoretical understanding of self-supervised learning The empirical success of contrastive learning has triggered a surge of theoretical explorations into the contrastive loss [2, 21, 22, 63, 64, 33, 69, 45, 29, 58, 27, 56].

Wang & Isola [68] shed light on the optimal solutions of the InfoNCE loss, decomposing it as alignment term and uniformity term, contributing to a deeper comprehension of self-supervised learning. In HaoChen et al. [21], Shen et al. [54], Wang et al. [69], Tan et al. [56], self-supervised learning methods are examined from a spectral graph perspective. Alongside these black-box interpretations of contrastive learning, Saunshi et al. [52], HaoChen & Ma [20] argue that inductive bias also has significant influences on the downstream performance of self-supervised learning. Cabannes et al. [7] introduces a theoretical framework that elucidates the intricate relationship among the selection of data augmentation, the design of network architecture, and the training algorithm.

Various theoretical studies have also investigated non-contrastive methods for self-supervised learning [71, 61, 18, 5, 66, 49, 57, 34]. Garrido et al. [18] establishes the duality between contrastive and non-contrastive methods. Balestriero & LeCun [5] reveals the connections between variants of SimCLR, Barlow Twins, and VICReg to ISOMAP, Canonical Correlation Analysis, and Laplacian Eigenmaps, respectively. The fact that a method like SimSiam does not collapse is studied in Tian et al. [61]. The loss landscape of SimSiam is also compared to SimCLR’s in Pokle et al. [49], which shows that it learns bad minima. A variant of Barlow Twins’ criterion is also linked to a variant of HSIC in Tsai et al. [66]. The use of data augmentation in sample-contrastive learning has also been studied from a theoretical standpoint in Huang et al. [29], Wen & Li [70].

Neural collapse and dimensional collapse Papayan et al. [47] describe the intriguing phenomenon of Neural Collapse (NC), which manifests when training a classification network with cross-entropy loss. This phenomenon can be summarized that all the features of a single class converge to the mean of these features. In addition, the class-means form a simplex equiangular tight frame (ETF). Galanti et al. [16] demonstrates that the NC phenomenon can facilitate some transfer learning tasks.

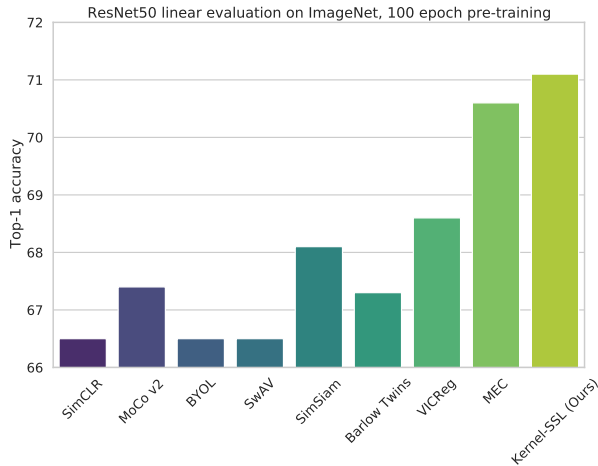


Figure 1: Linear evaluation results of Top-1 accuracy on ImageNet dataset with 100 epochs pre-training, using ResNet50 backbone.

However, potential concerns associated with neural collapse exist, as Ma et al. [40] posits that the total within-class features collapse may not be ideal for fine-grained classification tasks. Zhuo et al. [80] advocate for a comprehensive theoretical understanding of non-contrastive learning through the mechanism of rank differential. We briefly introduce NC and ETF in Appendix B.

3 Background

3.1 Reproducing Kernel Hilbert Space

Given two objects (e.g., images) $\mathbf{X}_i, \mathbf{X}_j \in X$, we can define a feature map $\mathbf{f} : X \rightarrow \mathcal{H}$ that projects these objects into an (maybe infinite-dimensional) high-dimensional feature space \mathcal{H} . A kernel function k measures the similarity between \mathbf{X}_i and \mathbf{X}_j as $k(\mathbf{X}_i, \mathbf{X}_j) \triangleq \langle \mathbf{f}(\mathbf{X}_i), \mathbf{f}(\mathbf{X}_j) \rangle_{\mathcal{H}}$.

Definition 3.1 (Reproducing kernel Hilbert space (RKHS)). A Hilbert space \mathcal{H} of \mathbb{R} -valued functions defined on a non-empty set X is a *reproducing kernel Hilbert space* if it has a reproducing kernel function $k : X \times X \rightarrow \mathbb{R}$ that satisfies

- $\forall \mathbf{X}_i \in X, k(\cdot, \mathbf{X}_i) \in \mathcal{H}$,
- $\forall \mathbf{X}_i \in X, \forall h \in \mathcal{H}, \langle h, k(\cdot, \mathbf{X}_i) \rangle_{\mathcal{H}} = h(\mathbf{X}_i)$.

Definition 3.2 (Mean embedding). Given a probability distribution p defined on X , we define the *mean embedding* of p in RKHS as

$$\mu_p \triangleq \int_x \mathbf{f}(x) dp(x), \quad (1)$$

Definition 3.3 (Covariance operator). For a probability distribution p defined on X , the *covariance operator* $\Sigma_p : \mathcal{H} \rightarrow \mathcal{H}$ in RKHS is defined as (* means conjugate transpose)

$$\Sigma_p \triangleq \int_x \mathbf{f}(x) \mathbf{f}(x)^* dp(x). \quad (2)$$

Interestingly, HSIC is exactly the Hilbert-Schmidt norm of the cross-covariance operator.

Definition 3.4 (Hilbert-Schmidt independence criterion (HSIC)). For probability distributions p and q defined on X and Y respectively, with the corresponding feature maps $\phi : X \rightarrow \mathcal{H}_X, \psi : Y \rightarrow \mathcal{H}_Y$, we define the Hilbert-Schmidt independence criterion (HSIC) as:

$$\text{HSIC}(X, Y) = \|\mathbb{E}[\phi(X)\psi(Y)^\top] - \mathbb{E}[\phi(X)]\mathbb{E}[\psi(Y)]^\top\|_{\text{HS}}^2. \quad (3)$$

3.2 Matrix divergence and kernel KL divergence

Definition 3.5 (Kernel KL divergence [3]). The Kullback-Leibler (KL) divergence, also known as kernel relative entropy, between two probability distributions p and q is defined as

$$D(\Sigma_p \parallel \Sigma_q) = \text{tr}[\Sigma_p(\log \Sigma_p - \log \Sigma_q)] \quad (4)$$

Empirical estimations of reproducing kernels can be represented by positive semi-definite matrices. The matrix (von Neumann) divergence is a Bregman divergence [1], serving as a measure of dissimilarity between two positive semi-definite matrices. It is defined in terms of the trace of their logarithmic difference. For a detailed introduction, please refer to Appendix A.3.

Definition 3.6 (Matrix (von Neumann) divergence). For two positive semi-positive matrices $\mathbf{P}, \mathbf{Q} \in \mathbb{R}^{n \times n}$, the matrix divergence is defined as

$$\text{MD}[\mathbf{P} : \mathbf{Q}] \triangleq \text{tr}(\mathbf{P} \log \mathbf{P} - \mathbf{P} \log \mathbf{Q} - \mathbf{P} + \mathbf{Q}) \quad (5)$$

3.3 Effective rank

Roy & Vetterli [51] introduced the concept of effective rank, which provides a real-valued extension of the classical rank.

Definition 3.7 (Effective rank [51]). The effective rank of a non-all-zero $A \in \mathbb{C}^{n \times n}$, denoted $\text{erank}(A)$, is defined as

$$\text{erank}(A) \triangleq \exp \{H(p_1, p_2, \dots, p_n)\}, \quad (6)$$

where $p_i = \frac{\sigma_i}{\sum_{k=1}^n \sigma_k}$, $\{\sigma_i | i = 1, \dots, n\}$ are the singular values of A , and H is the Shannon entropy defined as $H(p_1, p_2, \dots, p_n) = -\sum_{i=1}^n p_i \log p_i$, with the convention that $0 \log 0 \triangleq 0$.

The original definition applies to a complex-valued matrix $A \in \mathbb{C}^{m \times n}$. For a positive semi-definite matrix, its eigenvalues are equivalent to its singular values.

4 Understanding Non-Contrastive SSL from a Kernel Perspective

4.1 Notations

In non-contrastive learning, we consider an unlabeled dataset $\{x_i\}_{i=1}^n$ and aim to extract informative representations for each data point, which will later be utilized for various downstream tasks. This objective is typically accomplished via a pipeline involving two parameterized networks: the online network \mathbf{f}_θ and target network \mathbf{f}_ϕ . For a batch of B data points $\{x_i\}_{i=1}^B$, we can create different perspectives of them by randomly selecting an augmentation \mathcal{T} from a predefined set τ . Let $x'_i = \mathcal{T}(x_i)$ denote the representations passed through the online and target network as $\mathbf{z}_i^{(1)} = \mathbf{f}_\theta(x'_i) \in \mathbb{R}^d$ and $\mathbf{z}_i^{(2)} = \mathbf{f}_\phi(x_i) \in \mathbb{R}^d$. We define $\mathbf{Z}_1 = [\mathbf{z}_1^{(1)}, \dots, \mathbf{z}_B^{(1)}]$ and $\mathbf{Z}_2 = [\mathbf{z}_1^{(2)}, \dots, \mathbf{z}_B^{(2)}]$. The training loss is then expressed as $\mathcal{L} = \mathcal{L}(\mathbf{Z}_1, \mathbf{Z}_2)$.

4.2 On the equivalence between non-contrastive SSL and kernel uniformity

SimCLR [10] has been demonstrated to perform spectral clustering on a similarity graph [56] precisely by incorporating RKHS. Then a natural question arise, can we also use RKHS for characterizing the existing non-contrastive self-supervised learning methods?

In this section, we delve into a kernel-based understanding of existing non-contrastive self-supervised learning methods. Let's assume a kernel function k exists on the space of images, representing image similarity such that $k(x, x) = 1$. We denote the RKHS feature map from X to \mathcal{H} as \mathbf{f} and, for simplicity, we assume $\mathcal{H} \subseteq \mathbb{R}^d$.

Let's consider p_{data} , the probability distribution on X that describes the data distribution. We denote $q = p_{\text{data}} \circ \mathbf{f}^{-1}$ as the push-forward measure of p_{data} under the feature mapping \mathbf{f} (note that distribution q is supported on $\mathbf{f}(X)$). Given $\|\mathbf{f}(x)\|^2 = k(x, x) = 1$, it follows that $\mathbf{f}(X) \subseteq S^{d-1}$ (where S^{d-1} is the d -dimensional hypersphere with radius 1).

Applying the change-of-variables formula, we readily see the following lemma.

Lemma 4.1. *The expected value of q aligns exactly with the mean embedding of p . The auto-correlation matrix of q matches the covariance operator of p .*

A straightforward calculation yields the subsequent lemma.

Lemma 4.2. *Assume σ is the uniform distribution on S^{d-1} . The expected value of σ is 0 and the covariance (or auto-correlation matrix) of σ is $\frac{1}{d}\mathbf{I}_d$.*

When the kernel k is universal [42, 55], the covariance operator uniquely defines a distribution p_{data} [3]. By Lemma 4.1, we know that the auto-correlation matrix of q is the covariance operator of p_{data} . Thus based on the uniformity principle proposed by Wang & Isola [68], we want the (empirical) covariance operator of q to align with the (empirical) covariance operator of σ .

Matrix divergence and matrix cross-entropy (MCE) [77] depict a way of comparing two semi-positive definite (covariance) matrices. For a (random) batch of B data points $\{x_i\}_{i=1}^B$, denote $\mathbf{Z} = [\mathbf{f}(x_1), \dots, \mathbf{f}(x_B)]$. Recall the definition of MCE (see Appendix A.3), we now get the following loss function:

$$\text{MCE}\left(\frac{1}{d}\mathbf{I}_d, \frac{1}{B}\mathbf{Z}\mathbf{Z}^\top\right) = -\text{tr}\left(\frac{1}{d}\mathbf{I}_d \log\left(\frac{1}{B}\mathbf{Z}\mathbf{Z}^\top\right)\right) + \text{tr}\left(\frac{1}{B}\mathbf{Z}\mathbf{Z}^\top\right),$$

Given the potential numerical instability of the matrix logarithm, it’s beneficial to introduce a hyper-parameter $\lambda \geq 0$ to yield the regularized loss:

$$\text{MCE}\left(\frac{1}{d}\mathbf{I}_d + \lambda\mathbf{I}_d, \frac{1}{B}\mathbf{Z}\mathbf{Z}^\top + \lambda\mathbf{I}_d\right) = -\text{tr}\left(\left(\frac{1}{d}\mathbf{I}_d + \lambda\mathbf{I}_d\right)\log\left(\frac{1}{B}\mathbf{Z}\mathbf{Z}^\top + \lambda\mathbf{I}_d\right)\right) + \text{tr}\left(\frac{1}{B}\mathbf{Z}\mathbf{Z}^\top + \lambda\mathbf{I}_d\right),$$

Given that each $\mathbf{f}(x_i)$ resides on the hypersphere S^{d-1} , $\frac{1}{B}\mathbf{Z}\mathbf{Z}^\top$ has a constant trace of 1 (for l_2 normalized representations \mathbf{z}_i , since $\text{tr}(\mathbf{Z}\mathbf{Z}^\top) = \text{tr}(\mathbf{Z}^\top\mathbf{Z})$). Thus, upon simplifying the constant, the preceding loss equals the following:

$$\min -\text{tr}\log\left(\frac{1}{B}\mathbf{Z}\mathbf{Z}^\top + \lambda\mathbf{I}_d\right),$$

As we expect the online and target network to approximate the feature map \mathbf{f} , in practice, we can use cross-correlation between \mathbf{Z}_1 and \mathbf{Z}_2 to approximate $\mathbf{Z}\mathbf{Z}^\top$, thus getting the empirical loss as follows:

$$\min -\text{tr}\log\left(\frac{1}{B}\mathbf{Z}_1\mathbf{Z}_2^\top + \lambda\mathbf{I}_d\right), \quad (7)$$

Remark. This MCE formulation is closely related to Total Coding Rate (TCR) [41, 37, 62], which is grounded in lossy data coding and compression theory (since $\text{tr}\log(\cdot) = \log\det(\cdot)$):

$$R(Z) \triangleq \frac{1}{2}\log\det\left(\mathbf{I} + \frac{d}{b\epsilon^2}\mathbf{Z}\mathbf{Z}^\top\right) = \frac{1}{2}\text{tr}\log\left(\mathbf{I} + \frac{d}{b\epsilon^2}\mathbf{Z}\mathbf{Z}^\top\right),$$

Interestingly, this also recovers the Maximal Entropy Coding (MEC) loss given by Liu et al. [38]:

$$\mathcal{L}_{\text{MEC}} \triangleq -\mu\log\det\left(\mathbf{I}_b + \frac{d}{b\epsilon^2}\mathbf{Z}_1^\top\mathbf{Z}_2\right) = -\mu\log\det\left(\mathbf{I}_d + \frac{d}{b\epsilon^2}\mathbf{Z}_1\mathbf{Z}_2^\top\right),$$

As demonstrated by Liu et al. [38] using Taylor expansion, this formulation unifies BYOL (1st-order), SimSiam (1st-order), and Barlow Twins (2nd-order), providing a unified perspective of sample-wise and dimension-wise self-supervised learning [18].

4.3 Understanding the rank increasing phenomenon

Zhuo et al. [80] find an intriguing phenomenon that during the course of training, the effective rank of the feature covariance operator consistently increases. We offer an interpretation of this phenomenon from the perspective of reproducing kernel Hilbert space (RKHS). We consider the covariance operator $\Sigma_{p_{\text{data}}}$ associated with the distribution p_{data} . As we have mentioned earlier, many non-contrastive losses can be understood from the kernel uniformity viewpoint. As such, during training, $\Sigma_{p_{\text{data}}}$ is anticipated to progressively align more with \mathbf{I}_d . By Proposition A.2 in Appendix A.2 and the fact that \mathbf{I}_d achieves the maximal possible (matrix) entropy, the rank-increasing phenomenon can be well understood (For detailed discussions, please refer to Appendix A.2).

5 Measuring Dimensional Collapse

Papayan et al. [47] discuss the fascinating occurrence of neural collapse during the training of a supervised neural network utilizing cross-entropy loss for classification tasks. Contrastive learning may have similar effects of dimensional collapse due to its spectral clustering nature [56]. As non-contrastive learning can be seen as pursuing kernel uniformity, we are also interested in discovering the relationship between non-contrastive learning and dimensional collapse.

Fig. 2 illustrates that the non-contrastive method, Barlow Twins, exhibits greater intra-class variability than the contrastive method, SimCLR. However, for larger samples and classes (e.g., Fig 5 in Appendix C), this observation is qualitative explicit. To quantify this observation, we propose the introduction of metrics involving class-specific information to quantify dimensional collapse. These

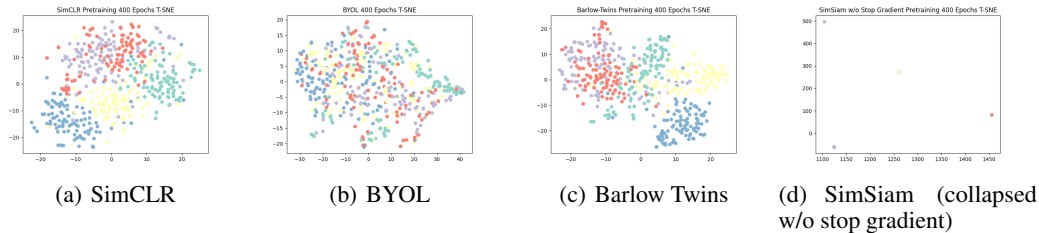


Figure 2: Visualization of feature representation for images in 5 different classes from CIFAR-100 dataset via t-SNE of various self-supervised learning methods. We find that SimCLR has larger inter-class variability than others, as the clusters seems more separable. For illustration, we also introduce a collapsed representation via SimSiam without stop gradient operation.

measures may enhance our understanding of the differences among supervised learning, contrastive, and non-contrastive SSL.

Assuming a total of K classes and n labeled samples $\{x_i, y_i\}_{i=1}^n$, denote the number of samples in each class c as n_c , i.e., $n_c = |\{i \mid y_i = c\}|$. We define the *intra-class effective rank* and *inter-class effective rank* as follows.

Definition 5.1 (Intra-class effective rank). Denote the class-mean vector of each class c as $\mu_c = \frac{1}{n_c} \sum_{y_i=c} \mathbf{f}(x_i)$,

and denote $\text{Cov}(\mathbf{f}(x) \mid y) = \frac{1}{n_y} \sum_{y_i=y} (\mathbf{f}(x_i) - \mu_y)(\mathbf{f}(x_i) - \mu_y)^\top$.

We define *intra-class effective rank* (intra-class erank) as

$$\frac{1}{K} \sum_{y \in [K]} \text{erank}(\text{Cov}(\mathbf{f}(x) \mid y)),$$

which can be viewed as an empirical approximation of $\mathbb{E}_{y \in [K]} [\text{erank}(\text{Cov}(\mathbf{f}(x) \mid y))]$, where x is drawn from p_{data} .

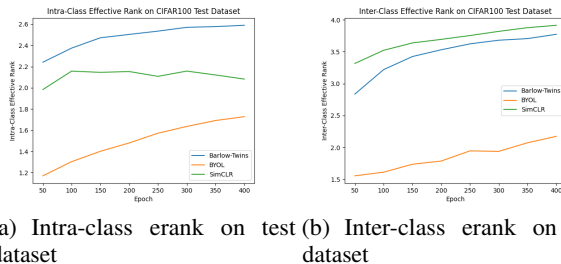
Definition 5.2 (Inter-class effective rank). Denote global mean of representation as $\mu_G = \frac{1}{n} \sum_{i \in [n]} \mathbf{f}(x_i)$, then we define *inter-class effective rank* (inter-class erank) as the effective rank of the covariance matrix of all C class-mean vectors,

$$\text{erank}\left[\frac{1}{K} \sum_{i \in [K]} (\mu_i - \mu_G)(\mu_i - \mu_G)^\top\right].$$

When class are balanced, intra-class erank is approximately $\text{erank}(\text{Cov}_{y \in [K]}(E[\mathbf{f}(x) \mid y]))$, where x is drawn from p_{data} .

Remark. These two metrics can be interpreted as an effective rank factorization of the two terms in the total covariance theorem. For more theoretical properties of effective rank and its connections to equiangular tight frame (ETF), please refer to Appendix A.4.

From illustrative examples shown in Fig. 3, we observe that SimCLR, as a contrastive method, exhibits a consistent decrease in intra-class effective rank during training. This empirical evidence corroborates the spectral clustering interpretation of contrastive learning. On the contrary, non-contrastive methods like BYOL and Barlow Twins, owing to the inherent property of kernel-uniformity loss (and its low-order Taylor approximations) tending towards a uniform distribution, exhibit larger intra-class effective ranks that continue to increase during training. Regarding the inter-class effective rank, a metric for global class-means effective rank, all three methods show a consistent increase.



(a) Intra-class erank on test dataset (b) Inter-class erank on test dataset

Figure 3: Intra-class effective rank and inter-class effective rank. It is obvious that intra-class effective rank continues to grow for BYOL or Barlow Twins, but not for SimCLR.

6 Kernel Alignment and Kernel Uniformity Framework for Self-Supervised Learning

See Fig. 4, we propose matrix cross-entropy (MCE) as a (class-agnostic) metric that can capture the tendency of dimensional collapse, since the equivalence between the logarithm of effective rank and matrix entropy. Other statistical metrics like RV-coefficient and simple matrix correlation may not capture the fully collapsed cases well.

When kernel k is universal, the mean embedding and covariance operator uniquely determined a distribution p_{data} . From the uniformity principle, we would like the mean embedding of p_{data} equals to 0 and the covariance operator equals to $\frac{1}{d}\mathbf{I}_d$.

As we also want to align the mean embedding, a direct way is to center the embeddings. The following theorem shows that optimizing covariance matrix uniformity may full-fill both mean and covariance embeddings.

Theorem 6.1. *Assume data distributed on the unit hypersphere S^{d-1} and the trace of the covariance matrix is at least one. Then when the covariance matrix has (maximal possible) effective rank d , the expected value will be 0 and the covariance matrix will be $\frac{1}{d}\mathbf{I}_d$.*

Proof. Dote the random vector $\mathbf{Z} = [\mathbf{z}_1, \dots, \mathbf{z}_d]^\top$ as a distribution on S^{d-1} . When the effective rank of the covariance matrix is maximized, the covariance matrix will have d equal eigenvalues. Then from the orthonormal standard form, the covariance matrix will be $\beta\mathbf{I}_d$, where β is a constant. As the covariance matrix $\text{Cov}(\mathbf{Z}) = \mathbb{E}(\mathbf{Z}\mathbf{Z}^\top) - \mathbb{E}(\mathbf{Z})\mathbb{E}(\mathbf{Z})^\top$. Then taking trace will give $1 \leq 1 - \sum_{i=1}^d \mathbb{E}(\mathbf{z}_i)^2 \leq 1$. Then the conclusion reveals. \square

Lemma 6.2. *Suppose $\mathbf{Z}_1, \mathbf{Z}_2 \in \mathbb{R}^{d \times B}$, where d is the dimensionality of the data and B is the number of samples. Then the cross-covariance matrix $\mathbf{C}(\mathbf{Z}_1, \mathbf{Z}_2)$ can be represented as*

$$\mathbf{C}(\mathbf{Z}_1, \mathbf{Z}_2) = \frac{1}{B-1} \mathbf{Z}_1 \mathbf{H}_B \mathbf{Z}_2^\top,$$

Proof. Please refer to Appendix A.1. \square

As discussed in the previous section, we can adopt the following loss as kernel uniformity:

$$\mathcal{L}_{\text{Kernel-uniformity}} = -\text{tr}\left(\frac{1}{d}\mathbf{I}_d \log\left(\frac{1}{B-1} \mathbf{Z}_1 \mathbf{H}_B \mathbf{Z}_2^\top\right)\right), \quad (8)$$

As for ease of optimization, we may add a regularization term $\lambda\mathbf{I}_d$ to the cross-covariance to make it non-singular. This makes it equivalent to MEC expect a mean normalization (representing mean embedding in RKHS).

Remark. Previous works such as Barlow Twins and VICReg also consider the covariance matrix regularization, but their theoretical initiation often builds upon Gaussian distribution assumptions. Another line of work based on Total Coding Rate (TCR) [41, 37, 38, 62] also proposes the covariance regularization on the perspective of lossy data compression. However, our formulation directly optimizes the (infinite-dimensional) mean embeddings and covariance operators of probability distributions beyond the Gaussian regime in RKHS.

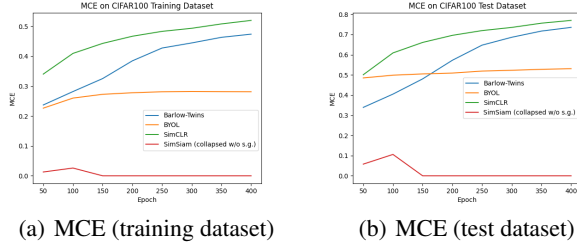


Figure 4: Visualization of MCE metric for evaluating the uniformity of representations during pre-training on CIFAR-100 dataset, (a) shows the metric on the training dataset while (b) shows the metric on the test dataset. We could find that successively pre-trained representations have MCE consistently increasing during training, demonstrating larger effective rank and more uniformly distributed feature representations.

6.1 Kernel alignment and kernel uniformity framework

From previous sections, we know that non-contrastive learning is different from contrastive learning, from the dimensional collapse and effective rank perspective. Now generalizing Wang & Isola [68]’s axiomatic understanding of contrastive learning, we propose the kernel alignment and kernel uniformity framework to improve self-supervised learning:

$$\mathcal{L}_{\text{Kernel-SSL}} = \mathcal{L}_{\text{Kernel-alignment}} + \mathcal{L}_{\text{Kernel-uniformity}}$$

where Kernel-alignment loss can be MCE, HSIC, or a linear combination of them:

$$\mathcal{L}_{\text{Kernel-alignment-MCE}} = -\text{tr}\left(\frac{1}{B-1}\mathbf{Z}_1\mathbf{H}_B\mathbf{Z}_1^\top \log\left(\frac{1}{B-1}\mathbf{Z}_2\mathbf{H}_B\mathbf{Z}_2^\top\right)\right), \quad (9)$$

$$\mathcal{L}_{\text{Kernel-alignment-HSIC}} = -\text{tr}\left(\frac{1}{(B-1)^2}\mathbf{Z}_1^\top\mathbf{Z}_1\mathbf{H}_B\mathbf{Z}_2^\top\mathbf{Z}_2\mathbf{H}_B\right), \quad (10)$$

Notably, MCE is a natural empirical estimator of Kernel KL divergence with theoretical guarantees and is easy to optimize (please refer to Appendix A.3).

7 Experiments

7.1 Implementation details

Pseudo-code. The pseudo-code for Kernel-SSL is shown as Algorithm 1 in Appendix C.

Dataset and data augmentations. We implement our proposed Kernel-SSL method on the self-supervised learning task of ImageNet ILSVRC-2012 [13] training dataset. We use precisely the same data augmentation protocols and hyperparameters with previous baselines such as BYOL [19], SimSiam [11] and MEC [38], etc. In detail, our augmentation protocol consists of random cropping, color jittering, color dropping (grayscale), left-right flipping, Gaussian blurring, and solarization. We augment each image twice to get two different views during each training iteration.

Architecture. Similar to MEC [38], we select one branch of the Siamese network as the online network and the other branch as the target network, updating the parameters using the exponential moving average method instead of loss backward. we use ResNet50 [23] without the last linear layer as the backbone encoder, whose output feature dimension is 2048. Then we use a three-layer MLP with BN(Batch Normalization) [30] and ReLU [44] as the projector after the encoder, and the projector maintains the feature dimension to be 2048 through three layers. For the online network, we apply an extra two-layer MLP with BN [30] and ReLU [44] with hidden dimension 512 and output dimension 2048.

Linear evaluation. We follow the standard linear evaluation protocol [10, 19, 11]. We freeze the parameters of the backbone encoder and connect a linear classification layer after it, and train the linear layer in the supervised setting. During the training process, each image is augmented by random cropping, resizing to 224×224 , and random horizontal flipping. And at test time, each image is resized to 256×256 and center cropped to 224×224 .

Linear evaluation of the Top-1 accuracy result pre-trained with 100 epochs on ImageNet [13] dataset was shown in Table 1. Notice that we use ResNet50 backbone as default for a fair comparison.

Method	Top-1 accuracy
SimCLR [10]	66.5
MoCo v2 [12]	67.4
BYOL [19]	66.5
SwAV [8]	66.5
SimSiam [11]	68.1
Barlow Twins [75]	67.3
VICReg [6]	68.6
MEC [38]	70.6
Kernel-SSL (Ours)	71.1

Table 1: Linear evaluation results on ImageNet dataset with 100 epochs pre-training, using ResNet50 backbone.

Remark. Using the representation theorem in RKHS ([53, 31]), we can derive linear probing as the canonical approach for the downstream task of image classification. A data-dependent generalization bound can also be derived accordingly [35].

Optimization and hyperparameters. For pre-training, we use SGD optimizer with 2048 batch size, 10^{-5} weight decay, 0.9 momentum, and 4.0 base learning rate, which is scheduled by cosine decay learning rate scheduler [39], to optimize the online network over 100 epochs. For the momentum used for the exponential moving average process, it is set to be 0.996 to 1 scheduled by another cosine scheduler. As for linear evaluation, we use LARS optimizer [74] with 4096 batch size, 0.9 momentum, no weight decay, and 0.03 base learning rate scheduled by cosine decay learning rate scheduler, to train the linear layer over 100 epochs, and report the performance of last epoch. For more on experiment details, please refer to Appendix C.

7.2 Ablation studies

Kernel-alignment loss. We also studied the changes that different Kernel-alignment losses bring to the performance of Kernel-SSL on linear evaluation task. We keep most of the settings in 7.1 unchanged, except the Kernel-alignment loss. The results are summarized in Table 7.2. From the table, we can see that MCE alignment loss brings significant performance improvement, and adding a small ratio of HSIC alignment loss can further improve the performance slightly.

Method	Top-1 accuracy
$\mathcal{L}_{\text{Kernel-uniformity}}$ only	70.86
$\mathcal{L}_{\text{Kernel-uniformity}} + 0.003 \cdot \mathcal{L}_{\text{Kernel-alignment-HSIC}}$	70.88
$\mathcal{L}_{\text{Kernel-uniformity}} + \mathcal{L}_{\text{Kernel-alignment-MCE}}$	71.00
$\mathcal{L}_{\text{Kernel-uniformity}} + \mathcal{L}_{\text{Kernel-alignment-MCE}} + 1 \cdot \mathcal{L}_{\text{Kernel-alignment-HSIC}}$	70.80
$\mathcal{L}_{\text{Kernel-uniformity}} + \mathcal{L}_{\text{Kernel-alignment-MCE}} + 0.003 \cdot \mathcal{L}_{\text{Kernel-alignment-HSIC}}$	71.08

Table 2: Results of different Kernel-alignment loss. As shown in the table, MCE alignment can greatly improve performance, while small HSIC alignment can further slightly improve accuracy.

As we mentioned in previous sections, empirically we add a regularization term $\lambda \mathbf{I}_d$ to the cross-covariance when calculating the Kernel-uniformity loss, and we set λ to 1 in our experiments. For our best results, we choose the Kernel-alignment loss as (we set η as 0.003)

$$\begin{aligned} \mathcal{L}_{\text{Kernel-alignment}} &= \mathcal{L}_{\text{Kernel-alignment-MCE}} + \eta \cdot \mathcal{L}_{\text{Kernel-alignment-HSIC}} \\ &= -\text{tr}\left(\frac{1}{B-1} \mathbf{Z}_1 \mathbf{H}_B \mathbf{Z}_1^T \log\left(\frac{1}{B-1} \mathbf{Z}_2 \mathbf{H}_B \mathbf{Z}_2^T\right)\right) \\ &\quad - \eta \cdot \text{tr}\left(\frac{1}{(B-1)^2} \mathbf{Z}_1^T \mathbf{Z}_1 \mathbf{H}_B \mathbf{Z}_2^T \mathbf{Z}_2 \mathbf{H}_B\right), \end{aligned}$$

In addition, it is difficult to calculate the logarithm of the matrix directly, so for all matrix logarithmic calculations, we perform Taylor expansion to the 4-th order to approximate the matrix logarithm as an alternative to direct calculation.

Remark. Based on HSIC, Tsai et al. [66] modify it to avoid trivial representations, propose the HSIC-SSL loss which resembles Barlow Twins, including diagonal and off-diagonal terms. Li et al. [36] proposes SSL-HSIC, maximizing dependence between the image identity (encoding as one-hot vectors) and representation of the augmented image. On the contrary, we directly optimize the HSIC between representations of different views (augmentations).

8 Conclusion

In this paper, we provide a kernel perspective for understanding the non-contrastive learning methods. Based on this perspective, we propose two metrics for measuring dimensional collapse for various learning methods, and introduce new loss functions with superior empirical performance. We are confident that our kernel perspective will not only offer a refined and alternative comprehension of self-supervised learning methods but will also act as a catalyst for the design of increasingly robust and effective algorithms in the future.

Acknowledgments

This work is supported by the Ministry of Science and Technology of the People’s Republic of China, the 2030 Innovation Megaprojects “Program on New Generation Artificial Intelligence” (Grant No. 2021AAA0150000).

References

- [1] Amari, S.-i. Information geometry of positive measures and positive-definite matrices: Decomposable dually flat structure. *Entropy*, 16(4):2131–2145, 2014. 3, 16
- [2] Arora, S., Khandeparkar, H., Khodak, M., Plevrakis, O., and Saunshi, N. A theoretical analysis of contrastive unsupervised representation learning. In *International Conference on Machine Learning*, 2019. 1, 2
- [3] Bach, F. Information theory with kernel methods. *IEEE Transactions on Information Theory*, 2022. 3, 4, 16
- [4] Bachman, P., Hjelm, R. D., and Buchwalter, W. Learning representations by maximizing mutual information across views. *arXiv preprint arXiv:1906.00910*, 2019. 2
- [5] Balestrieri, R. and LeCun, Y. Contrastive and non-contrastive self-supervised learning recover global and local spectral embedding methods. *arXiv preprint arXiv:2205.11508*, 2022. 1, 2
- [6] Bardes, A., Ponce, J., and LeCun, Y. Vicreg: Variance-invariance-covariance regularization for self-supervised learning. *arXiv preprint arXiv:2105.04906*, 2021. 1, 2, 8
- [7] Cabannes, V., Kiani, B. T., Balestrieri, R., LeCun, Y., and Bietti, A. The ssl interplay: Augmentations, inductive bias, and generalization. *arXiv preprint arXiv:2302.02774*, 2023. 2
- [8] Caron, M., Misra, I., Mairal, J., Goyal, P., Bojanowski, P., and Joulin, A. Unsupervised learning of visual features by contrasting cluster assignments. *Advances in Neural Information Processing Systems*, 33:9912–9924, 2020. 2, 8
- [9] Caron, M., Touvron, H., Misra, I., Jégou, H., Mairal, J., Bojanowski, P., and Joulin, A. Emerging properties in self-supervised vision transformers. In *Proceedings of the IEEE/CVF international conference on computer vision*, pp. 9650–9660, 2021. 1, 2
- [10] Chen, T., Kornblith, S., Norouzi, M., and Hinton, G. A simple framework for contrastive learning of visual representations. In *International Conference on Machine Learning*, pp. 1597–1607. PMLR, 2020. 1, 2, 4, 8, 18
- [11] Chen, X. and He, K. Exploring simple siamese representation learning. In *Proceedings of the IEEE/CVF conference on Computer Vision and Pattern Recognition*, pp. 15750–15758, 2021. 1, 2, 8, 18
- [12] Chen, X., Fan, H., Girshick, R., and He, K. Improved baselines with momentum contrastive learning. *arXiv preprint arXiv:2003.04297*, 2020. 8
- [13] Deng, J., Dong, W., Socher, R., Li, L.-J., Li, K., and Fei-Fei, L. Imagenet: A large-scale hierarchical image database. In *2009 IEEE conference on computer vision and pattern recognition*, pp. 248–255. Ieee, 2009. 8
- [14] Du, S. S., Zhai, X., Póczos, B., and Singh, A. Gradient descent provably optimizes over-parameterized neural networks. *arXiv preprint arXiv:1810.02054*, 2018. 17
- [15] Dubois, Y., Hashimoto, T., Ermon, S., and Liang, P. Improving self-supervised learning by characterizing idealized representations. *arXiv preprint arXiv:2209.06235*, 2022. 2

- [16] Galanti, T., György, A., and Hutter, M. On the role of neural collapse in transfer learning. *arXiv preprint arXiv:2112.15121*, 2021. 2
- [17] Gao, T., Yao, X., and Chen, D. Simcse: Simple contrastive learning of sentence embeddings. *arXiv preprint arXiv:2104.08821*, 2021. 2
- [18] Garrido, Q., Chen, Y., Bardes, A., Najman, L., and Lecun, Y. On the duality between contrastive and non-contrastive self-supervised learning. *arXiv preprint arXiv:2206.02574*, 2022. 1, 2, 5
- [19] Grill, J.-B., Strub, F., Altché, F., Tallec, C., Richemond, P., Buchatskaya, E., Doersch, C., Avila Pires, B., Guo, Z., Gheshlaghi Azar, M., et al. Bootstrap your own latent—a new approach to self-supervised learning. *Advances in Neural Information Processing Systems*, 33:21271–21284, 2020. 1, 8, 18
- [20] HaoChen, J. Z. and Ma, T. A theoretical study of inductive biases in contrastive learning. *arXiv preprint arXiv:2211.14699*, 2022. 2
- [21] HaoChen, J. Z., Wei, C., Gaidon, A., and Ma, T. Provable guarantees for self-supervised deep learning with spectral contrastive loss. *Advances in Neural Information Processing Systems*, 34:5000–5011, 2021. 1, 2
- [22] HaoChen, J. Z., Wei, C., Kumar, A., and Ma, T. Beyond separability: Analyzing the linear transferability of contrastive representations to related subpopulations. *Advances in Neural Information Processing Systems*, 2022. 1, 2
- [23] He, K., Zhang, X., Ren, S., and Sun, J. Deep residual learning for image recognition. *CoRR*, abs/1512.03385, 2015. URL <http://arxiv.org/abs/1512.03385>. 8
- [24] Henaff, O. Data-efficient image recognition with contrastive predictive coding. In *International Conference on Machine Learning*, pp. 4182–4192. PMLR, 2020. 2
- [25] Higham, N. J. *Functions of matrices: theory and computation*. SIAM, 2008. 16
- [26] Hjelm, R. D., Fedorov, A., Lavoie-Marchildon, S., Grewal, K., Bachman, P., Trischler, A., and Bengio, Y. Learning deep representations by mutual information estimation and maximization. In *International Conference on Learning Representations*, 2018. 2
- [27] Hu, T., Liu, Z., Zhou, F., Wang, W., and Huang, W. Your contrastive learning is secretly doing stochastic neighbor embedding. *arXiv preprint arXiv:2205.14814*, 2022. 1, 2
- [28] Hua, T. SimSiam. <https://github.com/PatrickHua/SimSiam>, 2021. 18
- [29] Huang, W., Yi, M., and Zhao, X. Towards the generalization of contrastive self-supervised learning. *arXiv preprint arXiv:2111.00743*, 2021. 1, 2
- [30] Ioffe, S. and Szegedy, C. Batch normalization: Accelerating deep network training by reducing internal covariate shift. *CoRR*, abs/1502.03167, 2015. URL <http://arxiv.org/abs/1502.03167>. 8
- [31] Kiani, B. T., Balestrieri, R., Chen, Y., Lloyd, S., and LeCun, Y. Joint embedding self-supervised learning in the kernel regime. *CoRR*, abs/2209.14884, 2022. 9
- [32] Krizhevsky, A., Hinton, G., et al. Learning multiple layers of features from tiny images. *Citeseer*, 2009. 18, 19
- [33] Lee, J. D., Lei, Q., Saunshi, N., and Zhuo, J. Predicting what you already know helps: Provable self-supervised learning. *arXiv preprint arXiv:2008.01064*, 2020. 1, 2
- [34] Lee, J. D., Lei, Q., Saunshi, N., and Zhuo, J. Predicting what you already know helps: Provable self-supervised learning. *Advances in Neural Information Processing Systems*, 34:309–323, 2021. 2
- [35] Lei, Y., Dogan, Ü., Zhou, D., and Kloft, M. Data-dependent generalization bounds for multi-class classification. *IEEE Trans. Inf. Theory*, 65(5):2995–3021, 2019. 9

- [36] Li, Y., Pogodin, R., Sutherland, D. J., and Gretton, A. Self-supervised learning with kernel dependence maximization. *Advances in Neural Information Processing Systems*, 34:15543–15556, 2021. 1, 2, 9
- [37] Li, Z., Chen, Y., LeCun, Y., and Sommer, F. T. Neural manifold clustering and embedding. *arXiv preprint arXiv:2201.10000*, 2022. 5, 7
- [38] Liu, X., Wang, Z., Li, Y.-L., and Wang, S. Self-supervised learning via maximum entropy coding. *Advances in Neural Information Processing Systems*, 35:34091–34105, 2022. 1, 5, 7, 8
- [39] Loshchilov, I. and Hutter, F. SGDR: stochastic gradient descent with restarts. *CoRR*, abs/1608.03983, 2016. URL <http://arxiv.org/abs/1608.03983>. 9
- [40] Ma, J., You, C., Reddi, S. J., Jayasumana, S., Jain, H., Yu, F., Chang, S.-F., and Kumar, S. Do we need neural collapse? learning diverse features for fine-grained and long-tail classification. *OpenReviewNet*, 2023. 3
- [41] Ma, Y., Derksen, H., Hong, W., and Wright, J. Segmentation of multivariate mixed data via lossy data coding and compression. *IEEE transactions on pattern analysis and machine intelligence*, 29(9):1546–1562, 2007. 5, 7
- [42] Micchelli, C. A., Xu, Y., and Zhang, H. Universal kernels. *Journal of Machine Learning Research*, 7(12), 2006. 4
- [43] Misra, I. and Maaten, L. v. d. Self-supervised learning of pretext-invariant representations. In *Proceedings of the IEEE/CVF Conference on Computer Vision and Pattern Recognition*, pp. 6707–6717, 2020. 2
- [44] Nair, V. and Hinton, G. E. Rectified linear units improve restricted boltzmann machines. In *International Conference on Machine Learning*, 2010. 8
- [45] Nozawa, K. and Sato, I. Understanding negative samples in instance discriminative self-supervised representation learning. *Advances in Neural Information Processing Systems*, 34: 5784–5797, 2021. 1, 2
- [46] Oord, A. v. d., Li, Y., and Vinyals, O. Representation learning with contrastive predictive coding. *arXiv preprint arXiv:1807.03748*, 2018. 1, 2
- [47] Pappayan, V., Han, X., and Donoho, D. L. Prevalence of neural collapse during the terminal phase of deep learning training. *Proceedings of the National Academy of Sciences*, 117(40): 24652–24663, 2020. 2, 5, 17, 18
- [48] Pedregosa, F., Varoquaux, G., Gramfort, A., Michel, V., Thirion, B., Grisel, O., Blondel, M., Prettenhofer, P., Weiss, R., Dubourg, V., et al. Scikit-learn: Machine learning in python. *Journal of machine learning research*, 12(Oct):2825–2830, 2011. 19
- [49] Pokle, A., Tian, J., Li, Y., and Risteski, A. Contrasting the landscape of contrastive and non-contrastive learning. *arXiv preprint arXiv:2203.15702*, 2022. 2
- [50] Robinson, J. D., Chuang, C.-Y., Sra, S., and Jegelka, S. Contrastive learning with hard negative samples. In *ICLR*, 2021. 2
- [51] Roy, O. and Vetterli, M. The effective rank: A measure of effective dimensionality. In *2007 15th European signal processing conference*, pp. 606–610. IEEE, 2007. 3, 4, 17
- [52] Saunshi, N., Ash, J., Goel, S., Misra, D., Zhang, C., Arora, S., Kakade, S., and Krishnamurthy, A. Understanding contrastive learning requires incorporating inductive biases. In *International Conference on Machine Learning*, pp. 19250–19286. PMLR, 2022. 2
- [53] Schölkopf, B., Herbrich, R., and Smola, A. J. A generalized representer theorem. In Helmbold, D. P. and Williamson, R. C. (eds.), *Computational Learning Theory, 14th Annual Conference on Computational Learning Theory, COLT 2001 and 5th European Conference on Computational Learning Theory, EuroCOLT 2001, Amsterdam, The Netherlands, July 16-19, 2001, Proceedings*, volume 2111 of *Lecture Notes in Computer Science*, pp. 416–426. Springer, 2001. 9

- [54] Shen, K., Jones, R. M., Kumar, A., Xie, S. M., HaoChen, J. Z., Ma, T., and Liang, P. Connect, not collapse: Explaining contrastive learning for unsupervised domain adaptation. In *International Conference on Machine Learning*, pp. 19847–19878. PMLR, 2022. 2
- [55] Sriperumbudur, B. K., Gretton, A., Fukumizu, K., Schölkopf, B., and Lanckriet, G. R. Hilbert space embeddings and metrics on probability measures. *The Journal of Machine Learning Research*, 11:1517–1561, 2010. 4
- [56] Tan, Z., Zhang, Y., Yang, J., and Yuan, Y. Contrastive learning is spectral clustering on similarity graph. *arXiv preprint arXiv:2303.15103*, 2023. 1, 2, 4, 5
- [57] Tao, C., Wang, H., Zhu, X., Dong, J., Song, S., Huang, G., and Dai, J. Exploring the equivalence of siamese self-supervised learning via a unified gradient framework. In *Proceedings of the IEEE/CVF Conference on Computer Vision and Pattern Recognition*, pp. 14431–14440, 2022. 2
- [58] Tian, Y. Deep contrastive learning is provably (almost) principal component analysis. *arXiv preprint arXiv:2201.12680*, 2022. 1, 2
- [59] Tian, Y., Krishnan, D., and Isola, P. Contrastive multiview coding. *arXiv preprint arXiv:1906.05849*, 2019. 2
- [60] Tian, Y., Sun, C., Poole, B., Krishnan, D., Schmid, C., and Isola, P. What makes for good views for contrastive learning. *arXiv preprint arXiv:2005.10243*, 2020. 2
- [61] Tian, Y., Chen, X., and Ganguli, S. Understanding self-supervised learning dynamics without contrastive pairs. In *International Conference on Machine Learning*, pp. 10268–10278. PMLR, 2021. 2
- [62] Tong, S., Chen, Y., Ma, Y., and Lecun, Y. Emp-ssl: Towards self-supervised learning in one training epoch. *arXiv preprint arXiv:2304.03977*, 2023. 5, 7
- [63] Tosh, C., Krishnamurthy, A., and Hsu, D. Contrastive estimation reveals topic posterior information to linear models. *arXiv:2003.02234*, 2020. 1, 2
- [64] Tosh, C., Krishnamurthy, A., and Hsu, D. Contrastive learning, multi-view redundancy, and linear models. In *Algorithmic Learning Theory*, pp. 1179–1206. PMLR, 2021. 1, 2
- [65] Tsai, Y. H., Bai, S., Morency, L., and Salakhutdinov, R. A note on connecting barlow twins with negative-sample-free contrastive learning. *CoRR*, abs/2104.13712, 2021. URL <https://arxiv.org/abs/2104.13712>. 18
- [66] Tsai, Y.-H. H., Bai, S., Morency, L.-P., and Salakhutdinov, R. A note on connecting barlow twins with negative-sample-free contrastive learning. *arXiv preprint arXiv:2104.13712*, 2021. 2, 9
- [67] van der Maaten, L. and Hinton, G. E. Visualizing data using t-sne. *Journal of Machine Learning Research*, 9:2579–2605, 2008. 19
- [68] Wang, T. and Isola, P. Understanding contrastive representation learning through alignment and uniformity on the hypersphere. In *International Conference on Machine Learning*, pp. 9929–9939. PMLR, 2020. 2, 4, 8
- [69] Wang, Y., Zhang, Q., Wang, Y., Yang, J., and Lin, Z. Chaos is a ladder: A new theoretical understanding of contrastive learning via augmentation overlap. *arXiv preprint arXiv:2203.13457*, 2022. 1, 2
- [70] Wen, Z. and Li, Y. Toward understanding the feature learning process of self-supervised contrastive learning. In *International Conference on Machine Learning*, pp. 11112–11122. PMLR, 2021. 2
- [71] Wen, Z. and Li, Y. The mechanism of prediction head in non-contrastive self-supervised learning. *arXiv preprint arXiv:2205.06226*, 2022. 2

- [72] Wu, Z., Xiong, Y., Yu, S. X., and Lin, D. Unsupervised feature learning via non-parametric instance discrimination. In *Proceedings of the IEEE Conference on Computer Vision and Pattern Recognition*, pp. 3733–3742, 2018. 2
- [73] Ye, M., Zhang, X., Yuen, P. C., and Chang, S.-F. Unsupervised embedding learning via invariant and spreading instance feature. In *Proceedings of the IEEE/CVF Conference on Computer Vision and Pattern Recognition*, pp. 6210–6219, 2019. 2
- [74] You, Y., Gitman, I., and Ginsburg, B. Scaling SGD batch size to 32k for imagenet training. *CoRR*, abs/1708.03888, 2017. URL <http://arxiv.org/abs/1708.03888>. 9
- [75] Zbontar, J., Jing, L., Misra, I., LeCun, Y., and Deny, S. Barlow twins: Self-supervised learning via redundancy reduction. In *International Conference on Machine Learning*, pp. 12310–12320. PMLR, 2021. 1, 2, 8, 18
- [76] Zhang, C., Bengio, S., Hardt, M., Recht, B., and Vinyals, O. Understanding deep learning (still) requires rethinking generalization. *Communications of the ACM*, 64(3):107–115, 2021. 17
- [77] Zhang, Y., Yang, J., Tan, Z., and Yuan, Y. Relationmatch: Matching in-batch relationships for semi-supervised learning. *arXiv preprint arXiv:2305.10397*, 2023. 4
- [78] Zhou, J., You, C., Li, X., Liu, K., Liu, S., Qu, Q., and Zhu, Z. Are all losses created equal: A neural collapse perspective. *arXiv preprint arXiv:2210.02192*, 2022. 18
- [79] Zhu, Z., Ding, T., Zhou, J., Li, X., You, C., Sulam, J., and Qu, Q. A geometric analysis of neural collapse with unconstrained features. *Advances in Neural Information Processing Systems*, 34: 29820–29834, 2021. 17, 18
- [80] Zhuo, Z., Wang, Y., Ma, J., and Wang, Y. Towards a unified theoretical understanding of non-contrastive learning via rank differential mechanism. In *The Eleventh International Conference on Learning Representations*, 2023. 3, 5, 15, 17

Author Contributions

Yifan Zhang discovered the relationship between kernel KL divergence and self-supervised learning methods, as well as the relationship between effective rank and matrix entropy. Yifan Zhang proposed the kernel-alignment and kernel-uniformity framework (Kernel-SSL method). Yifan Zhang wrote most part of the paper. Zhiqian Tan formalized the framework of kernel KL divergence, proposed the metric of dimensional collapse, and proved all the theorems. Jingqin Yang implemented all the experiments and wrote the experimental section. Yang Yuan polished the paper.

A Details on Proofs

A.1 Centering matrix and covariance matrix

Suppose $\mathbf{Z}_1, \mathbf{Z}_2 \in \mathbb{R}^{d \times B}$, where d is the dimensionality of the data and B is the number of samples. We want to express cross-covariance matrix $\mathbf{C}(\mathbf{Z}_1, \mathbf{Z}_2)$ using the centering matrix, denoted as $\mathbf{H}_B \triangleq \mathbf{I}_B - \frac{1}{B} \mathbf{1}_B \mathbf{1}_B^T$.

The centering matrix is used to center the data by subtracting the mean of each row. We can apply the centering matrix to \mathbf{Z}_1 and \mathbf{Z}_2 as follows:

$$\begin{aligned}\bar{\mathbf{Z}}_1 &= \mathbf{Z}_1 \mathbf{H}_B \\ \bar{\mathbf{Z}}_2 &= \mathbf{Z}_2 \mathbf{H}_B\end{aligned}$$

Now, we can compute the cross-covariance matrix $\mathbf{C}(\mathbf{Z}_1, \mathbf{Z}_2)$ using the centered data:

$$\mathbf{C}(\mathbf{Z}_1, \mathbf{Z}_2) = \frac{1}{B-1} \bar{\mathbf{Z}}_1 \bar{\mathbf{Z}}_2^T$$

In summary, the cross-covariance matrix $\mathbf{C}(\mathbf{Z}_1, \mathbf{Z}_2)$ using the centering matrix can be expressed as:

$$\mathbf{C}(\mathbf{Z}_1, \mathbf{Z}_2) = \frac{1}{B-1} (\mathbf{Z}_1 \mathbf{H}_B) (\mathbf{Z}_2 \mathbf{H}_B)^T$$

Given that the centering matrix \mathbf{H} is symmetric and idempotent, it satisfies the following properties:

1. Symmetric: $\mathbf{H} = \mathbf{H}^T$,
2. Idempotent: $\mathbf{H}^2 = \mathbf{H}$.

Using these properties, we can simplify the expression for the cross-covariance matrix as follows:

$$\mathbf{C}(\mathbf{Z}_1, \mathbf{Z}_2) = \frac{1}{B-1} (\mathbf{Z}_1 \mathbf{H}) (\mathbf{Z}_2 \mathbf{H})^T = \frac{1}{B-1} \mathbf{Z}_1 \mathbf{H}_B \mathbf{H}_B^T \mathbf{Z}_2^T$$

Since $\mathbf{H} = \mathbf{H}_B^T$ and $\mathbf{H}_B^2 = \mathbf{H}_B$, the expression becomes:

$$\mathbf{C}(\mathbf{Z}_1, \mathbf{Z}_2) = \frac{1}{B-1} \mathbf{Z}_1 \mathbf{H}_B^2 \mathbf{Z}_2^T = \frac{1}{B-1} \mathbf{Z}_1 \mathbf{H}_B \mathbf{Z}_2^T$$

So, the cross-covariance matrix $\mathbf{C}(\mathbf{Z}_1, \mathbf{Z}_2)$ using the centering matrix can be expressed more concisely as:

$$\mathbf{C}(\mathbf{Z}_1, \mathbf{Z}_2) = \frac{1}{B-1} \mathbf{Z}_1 \mathbf{H}_B \mathbf{Z}_2^T \tag{11}$$

A.2 Rank increasing phenomenon

Zhuo et al. [80] find an intriguing phenomenon that during the course of training, the effective rank of the feature (empirical) covariance operator consistently increases. We offer an interpretation of this phenomenon from the perspective of reproducing kernel Hilbert space (RKHS).

We consider the covariance operator $\Sigma_{p_{\text{data}}}$ associated with the distribution p_{data} . Let's assume x_1, \dots, x_B are independent and identically distributed (i.i.d.) samples from p_{data} , and a feature map $\mathbf{f} : \mathcal{X} \rightarrow \mathcal{H}$ is represented by a neural network. We introduce the natural estimator

$$\hat{\Sigma}_{p_{\text{data}}} = \frac{1}{B} \sum_{i=1}^B \mathbf{f}(x_i) \mathbf{f}(x_i)^\top,$$

The natural estimate for $\text{tr}[\Sigma_{p_{\text{data}}} \log \Sigma_{p_{\text{data}}}]$ is $\text{tr}[\hat{\Sigma}_{p_{\text{data}}} \log \hat{\Sigma}_{p_{\text{data}}}]$, which can be computed from the kernel matrix $\mathbf{K} \in \mathbb{R}^{B \times B}$ defined as $\mathbf{K}_{i,j} = k(x_i, x_j)$ with $1/\sqrt{B}$ convergence rate.

Proposition A.1 (Entropy for empirical covariance estimators [3]). *Given $\hat{\Sigma}_{p_{\text{data}}}$ and the above-defined kernel matrix, we have*

$$\text{tr} \left[-\hat{\Sigma}_{p_{\text{data}}} \log \hat{\Sigma}_{p_{\text{data}}} \right] = \text{tr} \left[-\frac{1}{B} \mathbf{K} \log \left(\frac{1}{B} \mathbf{K} \right) \right].$$

Proposition A.2 (Convergence properties of empirical covariance estimators [3]). *Under some mild conditions and assume p_{data} has a density with respect to the base measure which is greater than $\alpha < 1$. Assume that $c = \int_0^{+\infty} \sup_{x \in X} \langle \mathbf{f}(x), (\Sigma + \lambda I)^{-1} \mathbf{f}(x) \rangle^2 d\lambda$ is finite. Given i.i.d. samples x_1, \dots, x_B from p_{data} , we have:*

$$\mathbb{E} \left[\left| \text{tr} \left[\hat{\Sigma}_{p_{\text{data}}} \log \hat{\Sigma}_{p_{\text{data}}} \right] - \text{tr} \left[\Sigma_{p_{\text{data}}} \log \Sigma_{p_{\text{data}}} \right] \right| \right] \leq \frac{1 + c(8 \log B)^2}{B\alpha} + \frac{17}{\sqrt{B}} (2\sqrt{c} + \log B).$$

Note that as a consequence of Jensen's inequality, we always have $\mathbb{E} \left(\text{tr} \left[\hat{\Sigma}_{p_{\text{data}}} \log \hat{\Sigma}_{p_{\text{data}}} \right] \right) \geq \text{tr} \left[\Sigma_{p_{\text{data}}} \log \Sigma_{p_{\text{data}}} \right]$.

Note that the logarithm of the effective rank of the batch auto-correlation matrix is exactly the matrix entropy by Definition 3.7 and A.3. As we have mentioned earlier, many non-contrastive losses can be understood from the kernel uniformity viewpoint. As such, during training, $\Sigma_{p_{\text{data}}}$ is anticipated to progressively align more with \mathbf{I}_d . By Proposition A.2 and the fact that \mathbf{I}_d achieves the maximal possible (matrix) entropy, the rank-increasing phenomenon can be well understood.

A.3 Matrix divergence and kernel KL divergence

Definition A.3 (Matrix (von Neuman) entropy). For a positive semi-definite matrix $\mathbf{A} \in \mathbb{R}^{n \times n}$ which is not all-zero, we define the matrix (von Neumann) entropy as:

$$-\text{tr}(\mathbf{A} \log \mathbf{A}), \tag{12}$$

where we use matrix principal logarithm [25].

We propose to use empirical covariance estimators to capture kernel KL divergence. Proposition A.2 shows the $1/\sqrt{B}$ convergence rate for empirical covariance estimators.

Just like the reason for introducing classical cross-entropy is for the simplicity of its optimization compared to classical KL divergence, we introduce the matrix cross-entropy:

Definition A.4 (Matrix cross-entropy (MCE)). For two positive semi-positive matrices $\mathbf{P}, \mathbf{Q} \in \mathbb{R}^{n \times n}$, the matrix cross-entropy is defined as

$$\text{MCE}(\mathbf{P}, \mathbf{Q}) \triangleq \text{tr}(-\mathbf{P} \log \mathbf{Q} + \mathbf{Q}). \tag{13}$$

Theorem A.5 (Projection Theorem [1]). *Given a smooth submanifold, S , let \mathbf{P}_S be the minimizer of divergence from \mathbf{P} to S ,*

$$\mathbf{P}_S = \min_{\mathbf{Q} \in S} D[\mathbf{P} : \mathbf{Q}].$$

Then, \mathbf{P}_S is the η -geodesic projection of \mathbf{P} to S , that is the η -geodesic connecting \mathbf{P} and \mathbf{P}_S is orthogonal to S .

The projection theorem gives the minimization property for MCE:

Proposition A.6 (Minimization property).

$$\text{argmin}_{\mathbf{Q} \succ 0} \text{MCE}(\mathbf{P}, \mathbf{Q}) = \mathbf{P}. \tag{14}$$

A.4 Effective rank and equiangular tight frame (ETF)

We now present some theoretical properties of effective rank and its connections to an equiangular tight frame (ETF). The following theorem suggests that a larger effective rank of the Gram matrix is beneficial for expressiveness.

Theorem A.7 (Maximize effective rank forms a equiangular tight frame (ETF)). *For K vectors \mathbf{z}_i ($1 \leq i \leq K$), each lying on S^{d-1} . Assuming the latent dimension d satisfies $d \geq K$ and the mean of \mathbf{z}_i is $\mathbf{0}$, denote $\mathbf{Z} = [\mathbf{z}_1, \dots, \mathbf{z}_K]$. If the Gram matrix $\mathbf{Z}^\top \mathbf{Z}$ has an effective rank of $K - 1$, it implies the existence of an equiangular tight frame (ETF) in the orthonormal span of \mathbf{z}_i . Conversely, the Gram matrix of any ETF has an effective rank of $K - 1$.*

Proof. Since the mean vector is $\mathbf{0}$, the Gram matrix can have an effective rank of at most $K - 1$. By Property 1 in [51], we deduce that the Gram matrix $\mathbf{Z}^\top \mathbf{Z}$ has $K - 1$ equal eigenvalues and one eigenvalue equal to 0.

The trace of the Gram matrix equals K because \mathbf{z}_i lies on S^{d-1} . Hence, the Gram matrix has $K - 1$ equal eigenvalues of $\frac{K}{K-1}$ and one eigenvalue of 0. Therefore, the Gram matrix shares the same eigenvalues (spectrum) as $\frac{K}{K-1} \mathbf{H}_K$, where \mathbf{H}_K is the centering matrix $\mathbf{I}_K - \frac{1}{K} \mathbf{1}_K \mathbf{1}_K^\top$.

Given the orthonormal standard form, there exists an orthonormal matrix $\mathbf{Q} \in \mathbf{R}^{K \times K}$ such that $\mathbf{Q}^\top (\mathbf{Z}^\top \mathbf{Z}) \mathbf{Q} = \frac{K}{K-1} \mathbf{H}_K$. According to Lemma 11 in Pappas et al. [47], $\mathbf{Z} \mathbf{Q}$ constitutes an ETF. As $\mathbf{Z} \mathbf{Q}$ directly represents the orthonormal span of \mathbf{Z} 's column space, the conclusion follows. \square

Gram matrix plays a key role in connecting our metric with Section 4.3, i.e., understanding the rank-increasing phenomenon.

Theorem A.8. *The effective rank of the total sample Gram matrix can be effectively estimated by batch.*

Proof. Note scaling does not change effective rank. Change the order of $\mathbf{Z}^\top \mathbf{Z}$ to $\mathbf{Z} \mathbf{Z}^\top$, then can rewrite self-correlation as the empirical estimation of expected self-correlation by samples in a batch. This explains the estimation given by Zhuo et al. [80]. \square

Interestingly, the following theorem connects our metrics with the Gram matrix.

Theorem A.9. *Assume the dataset is class balanced and the global mean is 0. Then effective rank of the covariance matrix of all K class-mean vectors is exactly the same as the effective rank of the Gram matrix.*

Proof. As $\mathbf{Z} \mathbf{Z}^\top$ and $\mathbf{Z}^\top \mathbf{Z}$ have the same non-zero eigenvalues, thus having the same effective rank. \square

B Neural Collapse and Dimensional Collapse

Feature representations acquired through a deep neural network employing a cross-entropy (CE) loss optimized by stochastic gradient descent, are capable of attaining zero loss [14] with arbitrary label assignments [76]. A phenomenon which known as neural collapse (NC) [47] is observed when training of the neural network continues beyond zero loss with CE. The NC phenomenon embodies the following characteristics [79]:

- **Variability collapse:** The intra-class variability of the final layer's features collapse to zero, signifying that all the features of a single class concentrate on the mean of these features for each class respectively.
- **Convergence to Simplex ETF:** Once centered at their global mean, the class-means are simultaneously linearly separable and maximally distant on a hypersphere. This results in the class-means forming a simplex equiangular tight frame (ETF), a symmetrical structure determined by a set of points on a hypersphere that is maximally distant and equiangular to each other.

- Convergence to self-duality: The linear classifiers, existing in the dual vector space of the class-means, converge to their respective class-mean and also construct a simplex ETF.
- Simplification to Nearest Class-Center (NCC): The linear classifiers behaviors similarly to the nearest class-mean decision rule.

Here we present the definition of standard K -Simplex ETF and general K -Simplex ETF [47].

Definition B.1 (K -Simplex ETF). A standard Simplex ETF is characterized as a set of points in \mathbb{R}^K , defined by the columns of

$$M = \sqrt{\frac{K}{K-1}} \left(I_K - \frac{1}{K} \mathbf{1}_K \mathbf{1}_K^\top \right),$$

where $I_K \in \mathbb{R}^{K \times K}$ is the identity matrix, and $\mathbf{1}_K \in \mathbb{R}^K$ represents a all-one vector. Consequently, we also obtain

$$M^\top M = MM^\top = \frac{K}{K-1} \left(I_K - \frac{1}{K} \mathbf{1}_K \mathbf{1}_K^\top \right).$$

Definition B.2 (General K -Simplex ETF). A general Simplex ETF is characterized as a set of points in \mathbb{R}^K , defined by the columns of

$$\tilde{M} = \alpha U M,$$

where $\alpha \in \mathbb{R}_+$ is a scale factor, and $U \in \mathbb{R}^{p \times K}$ ($p \geq K$) is a partial orthogonal matrix $U^\top U = I$.

Zhu et al. [79] further studied the problem using an unconstrained feature model that separates the topmost layers from the classifier of the neural network. They established that the conventional cross-entropy loss with weight decay presents a benign global landscape, where the only global minimizers are the Simplex ETFs and all other critical points are strict saddles exhibiting negative curvature directions.

The study was later extended [78], demonstrating through a global solution and landscape analysis that a wide range of loss functions, including commonly used label smoothing (LS) and focal loss (FL), display Neural Collapse. Therefore, all pertinent losses (i.e., CE, LS, FL, MSE) yield comparable features on training data.

C Details on Experiments

Taylor expansion order. We investigated the effect of the Taylor expansion order of matrix logarithm implementation on linear evaluation tasks. We keep most of the settings in 7.1 unchanged, except the Taylor expansion order. The results are summarized in Table C. As shown in the table, we found that Kernel-SSL performs best when the Taylor expansion order is 4, so we choose 4 as the default parameter.

Taylor expansion order	3	4	5
Top-1 accuracy	70.9	71.1	71.0

Table 3: Results of different Taylor expansion orders for Linear evaluation results

C.1 Experiments of dimensional collapse

We measure dimensional collapse on various self-supervised learning methods, including SimCLR [10], BYOL [19], Barlow Twins [75] and SimSiam [11] with or without stop gradient. We reproduce the above methods on the self-supervised learning task of CIFAR100 [32] dataset, using the open source implementations [65, 28] of the above methods tuned for CIFAR. After pre-training, we use the saved checkpoints to evaluate the results of these methods on different metrics.

We calculate the intra-class and inter-class effective rank directly by definition, while for MCE, we shuffle the testing dataset, import the data with 512 batch size, and finally output the average metrics of all batches.

Algorithm 1: PyTorch Pseudo-code for Kernel-SSL

```
#  $f$ : encoder network
#  $B$ : batch size
#  $\mathcal{L}_{\text{Kernel-uniformity}}$ : Kernel-uniformity loss
#  $\mathcal{L}_{\text{Kernel-alignment}}$ : Kernel-alignment loss
#  $\gamma$ : weight ratio between Kernel-alignment term and
Kernel-uniformity term
for  $X$  in loader:
    # augment a batch of  $B$  images in  $X$ 
     $X_1, X_2 = \text{aug}(X), \text{aug}(X)$ 

    # calculate  $l_2$  normalized embeddings
     $Z_1, Z_2 = f(X_1), f(X_2)$ 

    # calculate total coding rate and invariance loss
    uniformity_loss =  $\mathcal{L}_{\text{Kernel-uniformity}}(Z_1, Z_2)$ 
    alignment_loss =  $\mathcal{L}_{\text{Kernel-alignment}}(Z_1, Z_2)$ 

    # calculate loss
    loss = uniformity_loss +  $\gamma * \text{alignment\_loss}$ 

    # optimization step
    loss.backward()
    optimizer.step()
```

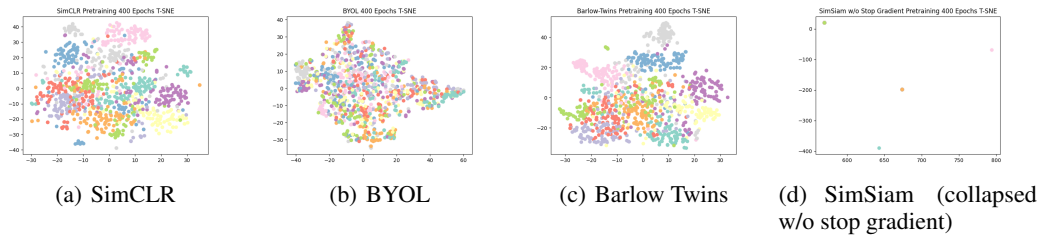


Figure 5: Visualization of feature representation for images in 10 different classes from CIFAR-100 dataset via t-SNE of various self-supervised learning methods. We find that in many categories, it is difficult to distinguish between two non-contrastive methods (BYOL, Barlow Twins) and contrastive method (SimCLR) by t-SNE.

We perform t-SNE [67] visualization on the last checkpoint of each method with the help of scikit-learn [48]. We use the default t-SNE [67] parameter of scikit-learn [48] and select the first 5 or 10 categories from 100 categories in CIFAR-100 [32] for visualization.